nature microbiology

SUPPLEMENTARY INFORMATION

https://doi.org/10.1038/s41564-019-0536-0

In the format provided by the authors and unedited.

Bacterial metabolic state more accurately predicts antibiotic lethality than growth rate

Allison J. Lopatkin[1,2,3], Jonathan M. Stokes[1,2,4], Erica J. Zheng[2,5], Jason H. Yang[1,2], Melissa K. Takahashi[1,6], Lingchong You[7] and James J. Collins[1,2,3,8,9,10]*

[1]Institute for Medical Engineering & Science and Department of Biological Engineering, Massachusetts Institute of Technology, Cambridge, MA, USA. [2]Infectious Disease and Microbiome Program, Broad Institute of MIT and Harvard, Cambridge, MA, USA. [3]Wyss Institute for Biologically Inspired Engineering, Harvard University, Boston, MA, USA. [4]Machine Learning for Pharmaceutical Discovery and Synthesis Consortium, Massachusetts Institute of Technology, Cambridge, MA, USA. [5]Program in Chemical Biology, Harvard University, Cambridge, MA, USA. [6]Department of Biology, California State University Northridge, Northridge, CA, USA. [7]Department of Biomedical Engineering, Duke University, Durham, NC, USA. [8]Department of Biological Engineering, Massachusetts Institute of Technology, Cambridge, MA, USA. [9]Synthetic Biology Center, Massachusetts Institute of Technology, Cambridge, MA, USA. [10]Harvard-MIT Program in Health Sciences and Technology, Cambridge, MA, USA. *e-mail: jimjc@mit.edu

Supplementary Information for

Bacterial metabolic state more accurately predicts antibiotic lethality than growth rate

Allison J. Lopatkin[1,2,3], Jonathan M. Stokes,[1,2] Erica J. Zheng[2,4], Jason H. Yang[1,2], Melissa K. Takahashi[1,5], Lingchong You[6], and James J. Collins[1,2,3,7,8,9,*]

[1]Institute for Medical Engineering & Science and Department of Biological Engineering, MIT; Cambridge, MA 02139; USA

[2]Infectious Disease and Microbiome Program; Broad Institute of MIT and Harvard; Cambridge, MA 02142; USA

[3]Wyss Institute for Biologically Inspired Engineering; Harvard University; Boston, MA 02115; USA

[4]Program in Chemical Biology, Harvard University; Cambridge, MA 02138; USA

[5]Department of Biology, California State University Northridge; Northridge, CA 91330; USA

[6]Department of Biomedical Engineering, Duke University; Durham, NC 27707; USA

[7]Department of Biological Engineering, Massachusetts Institute of Technology; Cambridge, MA 02139; USA

[8]Synthetic Biology Center, Massachusetts Institute of Technology; Cambridge, MA 02139; USA

[9]Harvard-MIT Program in Health Sciences and Technology; Cambridge, MA 02139; USA

*Corresponding author: jimjc@mit.edu

Supplementary Text

Background and motivation on the connection between growth and metabolism

Links between growth rate and antibiotic efficacy, or metabolic state and antibiotic efficacy, have primarily been studied separately[8–10]. For example, the lysis rate of β-lactam-treated cells has been shown to be robustly correlated with the growth rate[4,5]. Likewise, antibiotic efficacy can be promoted or suppressed by exploiting the active role of metabolic dysregulation in antibiotic-mediated cell death[6], such as by stimulating or inhibiting key aspects of cellular respiration[6,7]. Since bacterial growth inherently imposes a metabolic burden, it is likely that both aspects modulated previous observations of antibiotic efficacy. In some cases, the correlation between the two is straightforward; for example, cells in a metabolically dormant state that exhibit increased tolerance to antibiotic treatment have a drastically reduced growth rate[12,13]. However, the relationship between growth and metabolism can be skewed by nonlinear allocation of cellular resources between biomass production and other non-growth housekeeping functions (e.g., maintenance metabolism)[14,15]. Indeed, an organism's metabolic efficiency (e.g., ATP molecules required per biomass unit formed) depends on a host of factors including physiological state, nutrient composition, and other environmental parameters[16,17]. For example, rapidly growing cells counterintuitively exhibit overflow metabolism, wherein fermentation is used for energy production rather than the more efficient respiration[18–20]. Overall, strict coupling between substrate utilization and subsequent allocation between growth and respiration (e.g., anabolism and catabolism) often does not occur[21].

Intuition behind carbon and nitrogen metabolism in metabolic uncoupling

Classically, metabolic uncoupling describes scenarios where growth is nutrient-limited despite excess available energy[21–23]. As described in the main text, we refer to as 'coupled' any conditions under which growth and metabolism are both directionally correlated with increasing nutrient (Fig. 1a yellow); 'decoupled' describes any conditions under which growth is correlated to increasing nutrient, while metabolism is not (Fig. 1a blue)[21]. Specifically, the former refers to energy-limited growth, whereas the latter refers to nutrient-limited growth. When growth is energy-limited, any additional nutrient necessarily modulates both growth and

metabolism. However, when energy is sufficient, additional nutrients can modulate the overall cellular efficiency, allocating more resources to biomass accumulation and thus increasing growth rate. Achieving this requires two levels of control: overall energy limitation, which dictates the degree of coupling, and subsequent energy allocation, which determines nutrient-dependent growth rate.

To establish this, we focused on glucose as the primary energy source, since its bioenergetics are widely known: when glucose is dilute, efficiency is high (e.g., tight coupling between anabolism and catabolism), but when glucose is in excess, efficiency is low (e.g., energy spilling)[21,24]. Next, we reasoned that casamino acids (CAA) would be ideal for modulating the growth rate, since amino acid biosynthesis accounts for a substantial fraction of the cell's energy budget[25,26]. Intuitively, the high energetic burden of amino acid biosynthesis is alleviated by exogenous amino acid supplementation. Therefore, when growth is inefficient under high glucose, supplementation of CAA results in a decreased need for ATP directed toward amino acid synthesis. This allows for the more efficient allocation of glucose-derived ATP towards biomass, which in turn increases bacterial growth while cellular respiration stays overall constant[27–29].

Derivation for survival ratio

Paramount to this study was conditions that facilitated concurrent growth and metabolic activity. Thus, to ensure that growth is not a confounding factor in measuring its effect on lethality, we assume that untreated (N_C) cells grow exponentially at a rate μ, and antibiotic-treated (N_A) cells grow exponentially at a rate $f(\mu, A)$, where *f* is a generic growth function that may or may not depend on the antibiotic concentration A (Supplementary Eq. 1-2); we also assume cells die according to first order kinetics at a rate d:

$$\frac{dN_C}{dt} = N_C\mu \quad (1)$$

$$\frac{dN_A}{dt} = N_A(f(\mu, A) - dA) \quad (2)$$

These equations can be analytically solved (Supplementary Eq. 3-4).

$$\log(N_C) = t\mu + \log(N_0) \quad (3)$$

$$\log(N_A) = (f(\mu, A) - dA)t + \log(N_0) \quad (4)$$

Using this framework, we estimate survival fraction by normalizing the treated cell density by the control density, which is equivalent to subtracting the log-control CFU from the log-treated CFU (Supplementary Eq. 5). This is, by definition, an underestimate of the survival fraction, because the surviving cells in the control conditions are greater than the initial cell density (due to growth). This conservative assumption, in turn, emphasizes any effect that growth may have on the death rate d. In particular, we define survival S on the log domain as follows

$$\mathrm{S} = \log\left(\frac{\mathrm{N_A}}{\mathrm{N_C}}\right) = \log(N_A) - \log(N_C) = (f(\mu, A) - dA)t - \mu t$$

$$\%\mathrm{S} = \log\left(100 * \frac{\mathrm{N_A}}{\mathrm{N_C}}\right)$$

$$\%\mathrm{S} = 2 + \log(N_A) - \log(N_C)$$

$$\%\mathrm{S} = 2 + (f(\mu, A) - dA)t - \mu t \qquad 5.$$

Depending on the form of $f(\mu, A)$, we note that it is possible for growth during treatment to mask an observed growth-dependent death rate. Therefore, the validity of this definition depends on the form of $f(\mu, A)$. Thus, we investigate the two major cases:

a. Case 1: $\mu = 0$

$$S = (0 - dA)t - 0 = -dAt$$

In this case, there is no growth. Therefore, the survival percentage accurately reports on the true death rate.

b. Case 2: $\mu > 0$

I. $f(\mu, A) = \mu$.

$$S = t\mu - dAt - t\mu = -dAt$$

In this case, [A] does not affect growth rate. Thus, any increase in μ could counteract an increase in d. However, since we are subtracting N_C, this cancels out any possible confounding effect of growth.

II. $f(\mu, A) = 0$.

$$S = -dAt - t\mu$$

Here, [A] is sufficiently high to remove the effect of growth. In this case, the entire expression decreases as growth increases, which augments, rather than masks, any effects of increasing the death rate d on the survival ratio, as in Scenario A (and hence why survival may be an underestimate in certain conditions).

III. $f(\mu, A) = \mu \frac{k}{A+K}$

$$S = t\mu\left(\frac{K}{A+K}\right) - dAt - t\mu$$

In this case, [A] exerts some intermediate effect on growth. Here, we note that it is always the case that $t\mu\left(\frac{K}{A+K}\right) < \mu t$, and therefore as with scenario III., any increasing effect from growth will not mask any effects of increasing d.

Overall, by calculating survival fraction relative to the control population $\log(N) = \mu t + \log(N_0)$ rather than the initial condition N_0, this survival metric uniformly provides a lower bound on survival, and therefore an upper estimate of the killing rate. Furthermore, we show that growth is not sufficient to mask a killing effect; that conclusion is only strengthened when the antibiotic decreases the growth rate in addition to inducing killing. Finally, we note that these conclusions hold true at all antibiotic concentrations.

Supplementary Figures

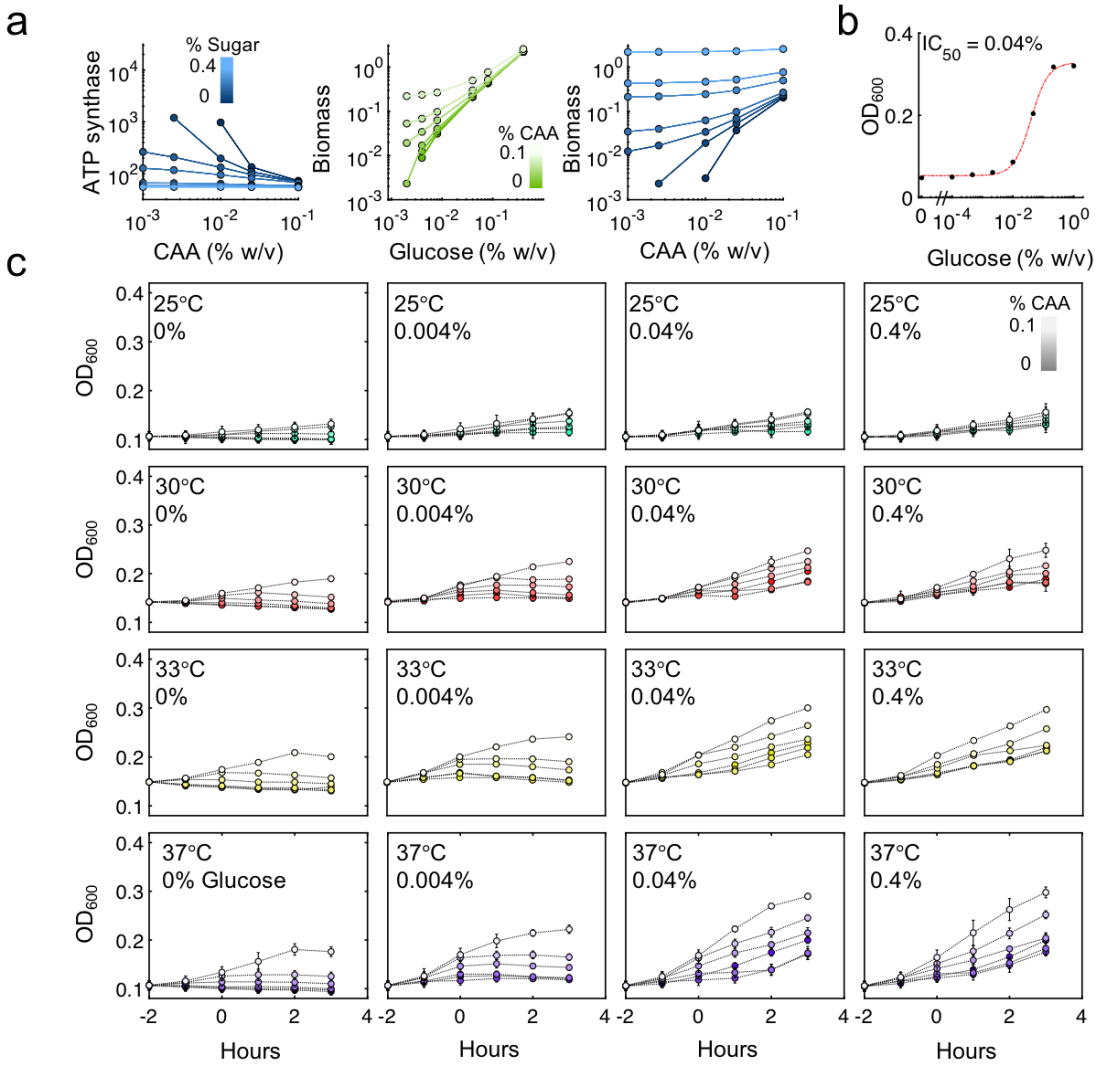

Supplementary Figure 1. Protocol validation

a. Flux balance analysis (FBA) reveals decoupled ATP and biomass. FBA simulations were performed using defined concentrations of glucose (0, 0.002, 0.004, 0.04, 0.08, 0.4% w/v) and CAA (0, 0.001, 0.0025, 0.01, 0.025, 0.1% w/v) and total ATP produced via ATP synthase was calculated across all conditions, normalized by the biomass. *Left:* Growth and metabolism were considered sufficiently decoupled at sugar concentrations where percent change in metabolic efficiency across [CAA] was >100-fold less than the corresponding change under coupled conditions (e.g., 0.04% glucose). *Middle* and *right* show biomass as a function of either glucose or CAA concentration. Glucose has a greater effect on increasing biomass than CAA.

b. Glucose IC_{50}. Glucose IC_{50} was determined by taking the steady-state biomass (OD_{600}) after 18 hours of growth for cells grown as described in Methods. Glucose concentrations were logarithmically spaced from 0.0001 to 1% (w/v), including 0. See Methods for curve fitting. Data points are the mean of three biological replicates and error bars indicate standard deviation.

c. Growth curves for all CAA, glucose, and temperature conditions. Cells were grown as described in Fig. 1b. Concentrations of glucose were 0, 0.004, 0.04, and 0,4% w/v, which span one order of magnitude above and below the IC_{50}, and are shown here increasing in panels from left to right. We used temperatures of 25, 30, 33, and 37°C, shown increasing in panels from top to bottom, and also correspond to teal, red, yellow, and purple, respectively. CAA concentrations of 0, 0.001, 0.0025, 0.01, 0.025, and 0.1% w/v were used for all subplots indicated by shading from dark to light for each respective color. The x-axis is in hours and y-axis is in OD_{600}. All data points are the mean OD_{600} of three biological replicates except for 33°C which is two; error bars indicating standard deviation are included when applicable.

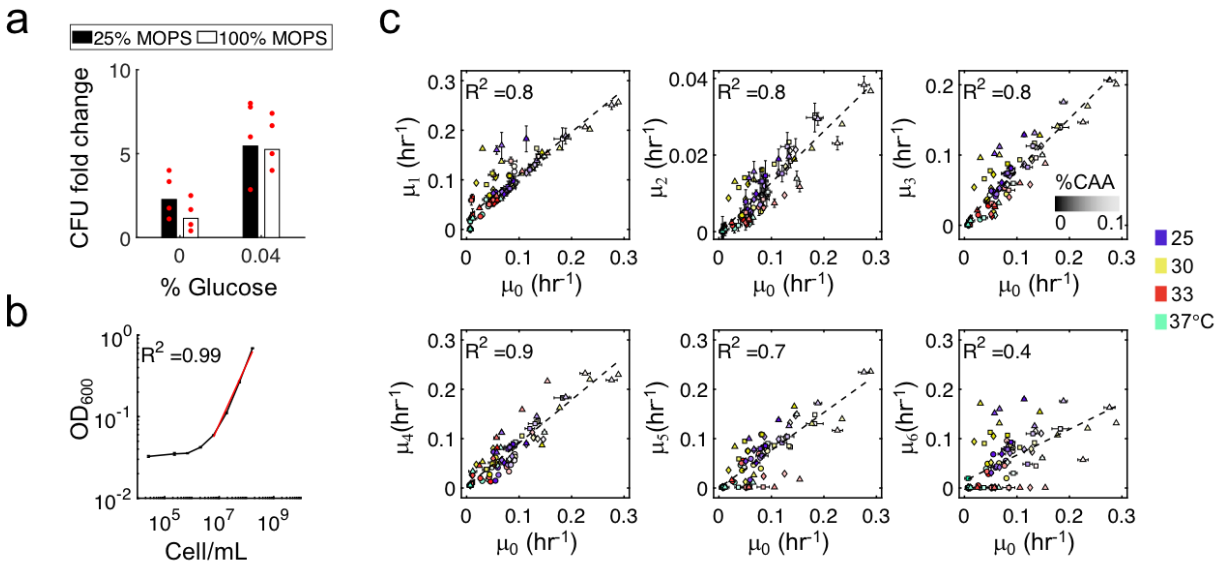

Supplementary Figure 2. Growth rate validation

a. Diluted MOPS does not change growth rate compared to standard MOPS. CFU was measured over the time corresponding to antibiotic treatment (from t=0 to 3 hours) in 100% MOPS or diluted 25% MOPS (in PBS), with either 0 or 0.04% glucose. CFU is statistically insignificantly different between the two MOPS conditions for 0% glucose (p=0.15) and 0.04% glucose (p=0.46) based on a two-tailed student t-test. Bar values are the mean fold change for four biological replicates; individual data points are shown in red.

b. Linear correlation between OD and CFU. Stationary-phase cells were suspended in 25% MOPS (diluted in PBS); 3-fold serial dilutions were performed and OD_{600} measured. CFU for the highest density well was measured using spread plating. The black line indicates the correlation between measured OD_{600} and CFU. The red line indicates the best-fit linear regression over the range of greatest linearity. Data points are the average of three biological replicates, and error bars indicate standard deviation.

c. All growth rate quantification methods are correlated. The x-axis, denoted μ_0, is the growth rate used throughout the main manuscript. Growth rates (μ_1-μ_6) are alternative definitions that demonstrate similar degrees of correlation, determined by a single variable linear regression fit. In particular, μ_1 uses an algorithmic detection to find the greatest portion of linear increase on a log-transformed growth curve as described in[30]; $\mu_2 = \frac{\mathrm{OD_{final}} - OD_{initial}}{\Delta t}$; $\mu_3 = \frac{\log(OD_{final}) - \log(OD_{initial})}{\Delta t}$; $\mu_4 = \frac{\log(OD_3) - \log(OD_1)}{\Delta t}$; $\mu_5 = \frac{\log(OD_5) - \log(OD_3)}{\Delta t}$; $\mu_6 = \frac{\log(OD_6) - \log(OD_4)}{\Delta t}$. We note certain conditions saturate the carrying capacity once time is sufficiently late; as a result, early growth rates are no longer predictive (e.g., μ_6). All data points are the mean of three biological replicates except for 33°C, which is two replicates; error bars of the standard deviation are included when applicable.

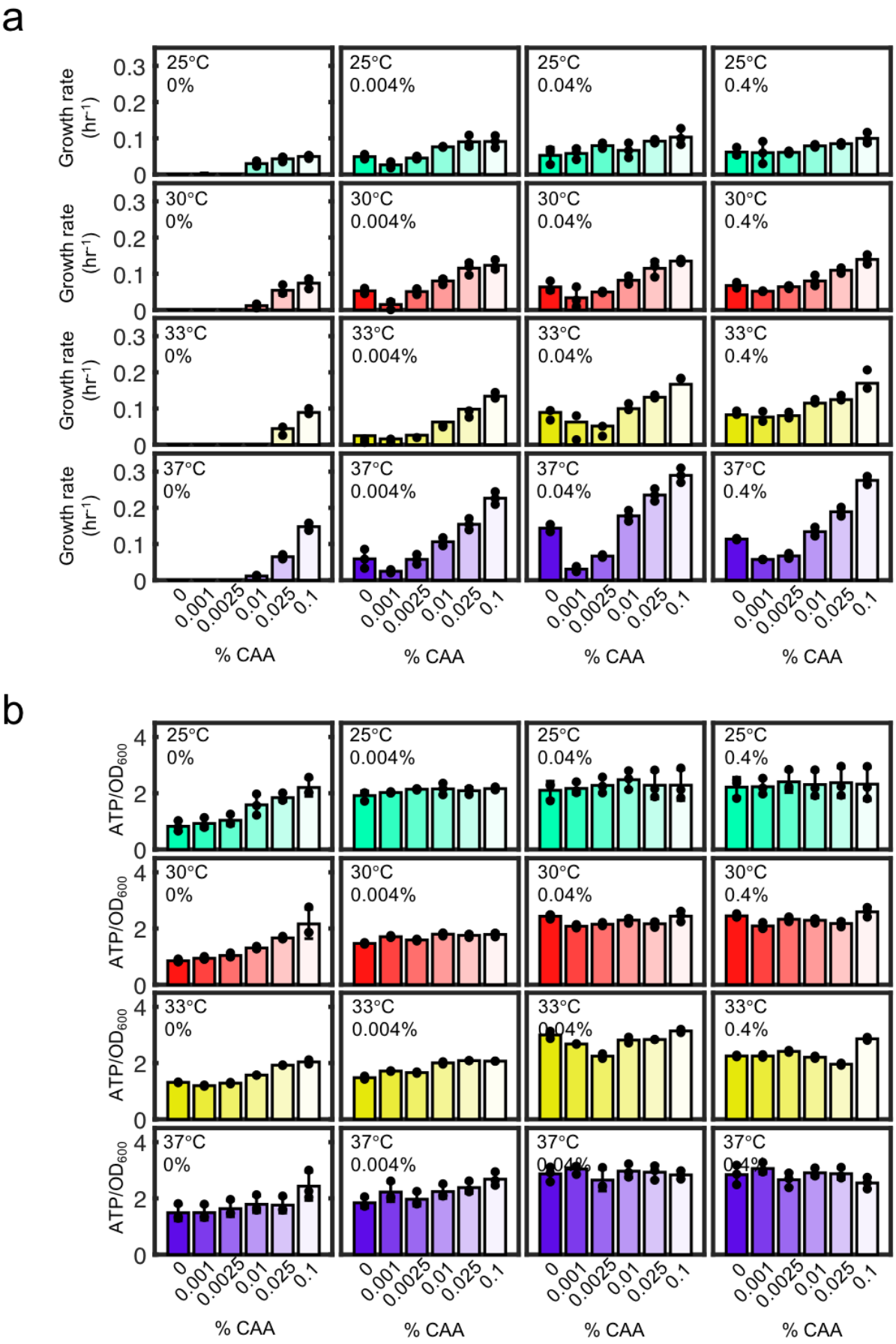

Supplementary Figure 3. Individual relationships between growth rate and ATP as a function of CAA. At low glucose (0 and 0.004%), both ATP/OD and growth rate are correlated with increasing CAA; once glucose is sufficiently high, ATP/OD no longer correlates. Bars are the mean of three biological replicates except for 33°C, which is two replicates. Error bars of standard deviation are included when applicable. Individual data points are shown in black.

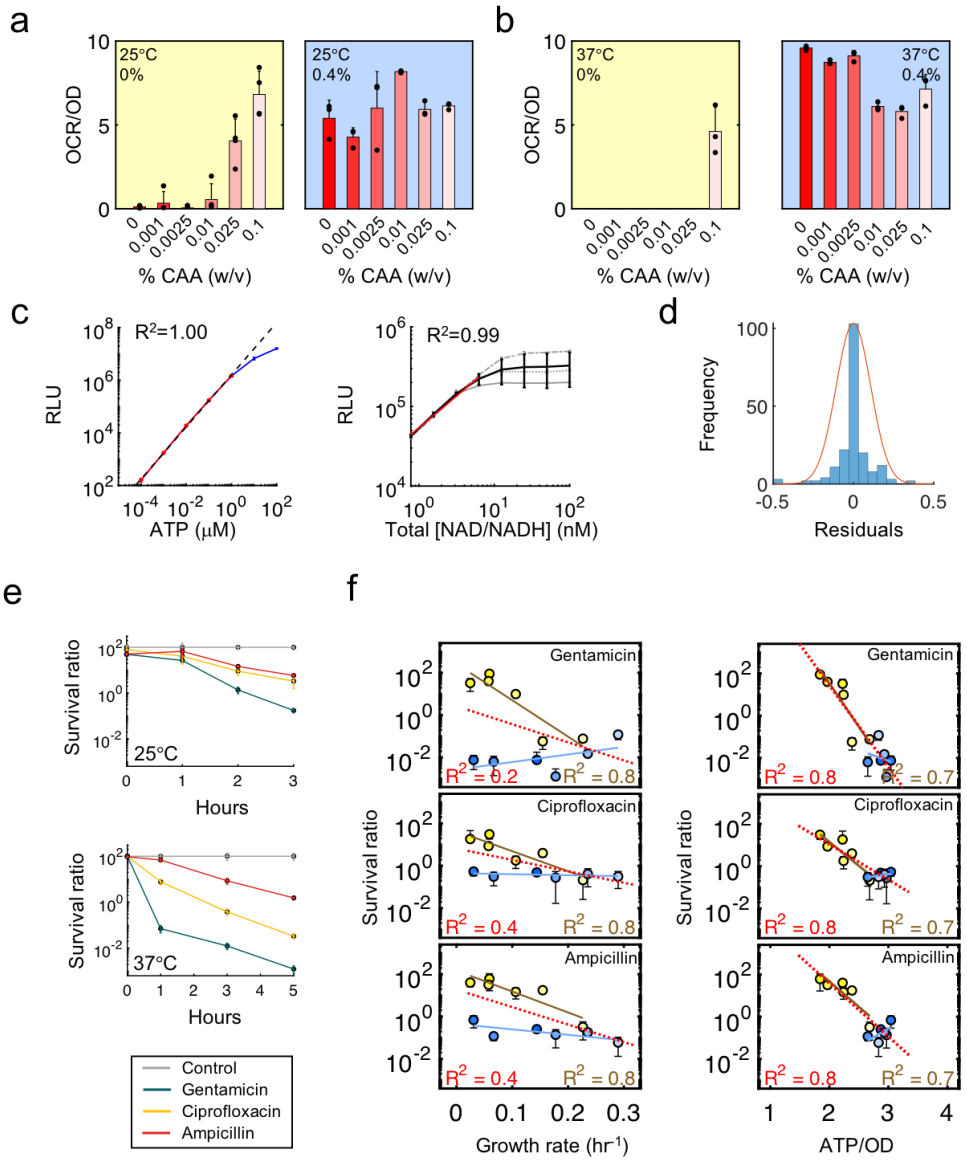

Supplementary Figure 4. Validation of experimental conditions

a-b. Oxygen consumption rate (OCR) at 25°C (a) and 37°C (b). Cells were treated with increasing [CAA] and either 0% (left) or 0.4% (right) glucose. OCR was measured at t_0 according to the manufacturer's instructions. Individual data points are in black; bars are the mean of three biological replicates and error bars show standard deviation. Yellow indicates coupled and blue indicates uncoupled conditions.

c. Standard curves for metabolism measurements. *Left: BacTiter-Glo standard curve.* Purified ATP (x-axis) was measured according to the manufacturer's instructions (RLU, y-axis). The linear portion of the black-dashed line was fit to the log-transformed exponential function (blue), and the linear range of ATP is highlighted in red. *Right: NAD/NADH standard curve.* Purified NAD and NADH were mixed in defined ratios, namely 1:1 (solid black line), 4:1 (dotted gray line), or 1:4 (solid gray line). The luminescence values obtained was multiplied by the respective dilution factor, resulting in a collapse over a specified linear range. This portion was fit to a linear regression. Solid red line indicates fit.

d. Residuals are normally distributed. The distribution is shown for residuals obtained from the linear regressions in Fig. 1c for both growth rate and ATP/OD. Red curve is scaled normal distribution.

e. Exponential killing. Survival was quantified at 1, 3, and 5 hours for 37°C, or 1, 2, and 3 for 25°C. Data are the average survival of four biological replicates; error bars indicate the standard deviation.

f. Antibiotic lethality is correlated with intracellular ATP. Survival was measured for gentamicin, ampicillin, and ciprofloxacin) at 2X MIC, and plotted against growth rate (*left*) and ATP/OD (*right*). Shading (dark to light) indicates increasing CAA. Survival data are the average of four biological replicates, and error bars indicate the standard deviation. Yellow and blue lines represent linear regressions for coupled and uncoupled conditions, respectively; red line is the linear regression for all data points combined. R^2 values are colored according to their corresponding conditions.

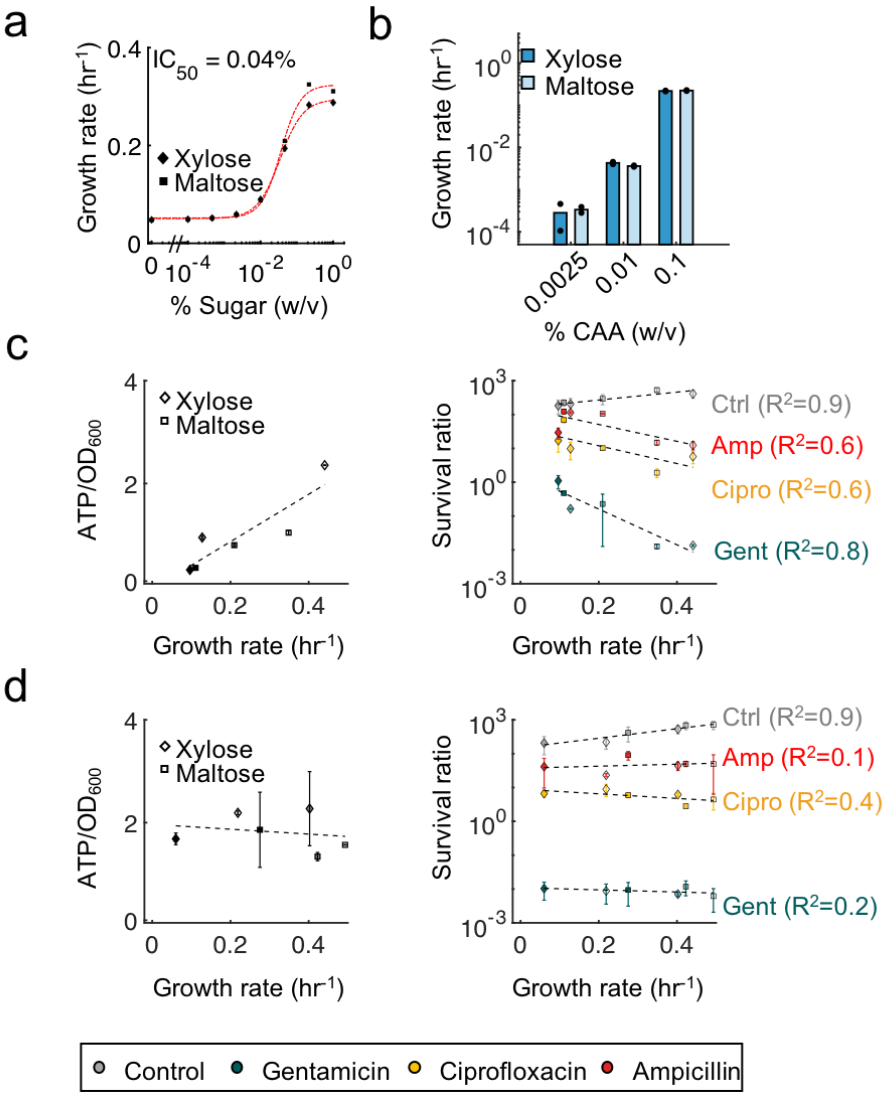

Supplementary Figure 5. Generality for xylose and maltose

a. Maltose and xylose IC_{50}. IC_{50} of either xylose (diamonds) or maltose (squares) was determined by taking the steady-state biomass (OD_{600}) after 18 hours of growth for logarithmically spaced [sugar] from 0.0001 to 1% (w/v). See Methods for curve fitting.

b. CAA-dependent growth rates for xylose and maltose growth. Growth rates were quantified by taking the log-transformed slope of the linearly increasing region, analogously to (a).

Data from (a) and (b) are the mean of two biological replicates; both data points are shown in black in (b).

c. Survival depends on growth rate when coupled to metabolism for alternative sugars. *Left:* Cells were harvested as described in Methods, supplemented with growth-permitting CAA concentrations (0.0025, 0.01, and 0.1% w/v), and grown at 37°C. Growth rate and intracellular ATP are coupled (slope=4.5, SE=1.3) for increasing CAA (shaded gray). *Right:* Survival is inversely correlated with growth rate for gentamicin (slope=-12.2, SE=2.3), ciprofloxacin (slope=-6.05, SE=2.9), and ampicillin (slope=-5.74, SE=2.4) at 2X MIC. Survival is quantified after four hours using 100% MOPS media. During the treatment, xylose and maltose are both 0%.

d. Survival is independent of growth rate when decoupled from metabolism for alternative sugars. Conditions identical to © plus 0.04% xylose or maltose during the treatment. *Left:* Growth rate and ATP are decoupled (slope=-0.31, SE=0.62). *Right:* Survival is independent of growth rate for gentamicin (slope=-0.7, SE=0.7), ciprofloxacin (slope=-1.6, SE=1.00), and ampicillin (slope=0.7, SE=1.33) at 2X MIC. Survival is quantified after four hours using 100% MOPS media.

Data in (c) and (d) are the mean of three biological replicates; error bar is the standard deviation. Shading (dark to light) indicates increasing CAA. Correlations were fit using a single variable linear regression model; conditions were deemed significant analogously to main dataset (e.g., slope estimate being statistically equal to zero defined by 2X standard error, SE).

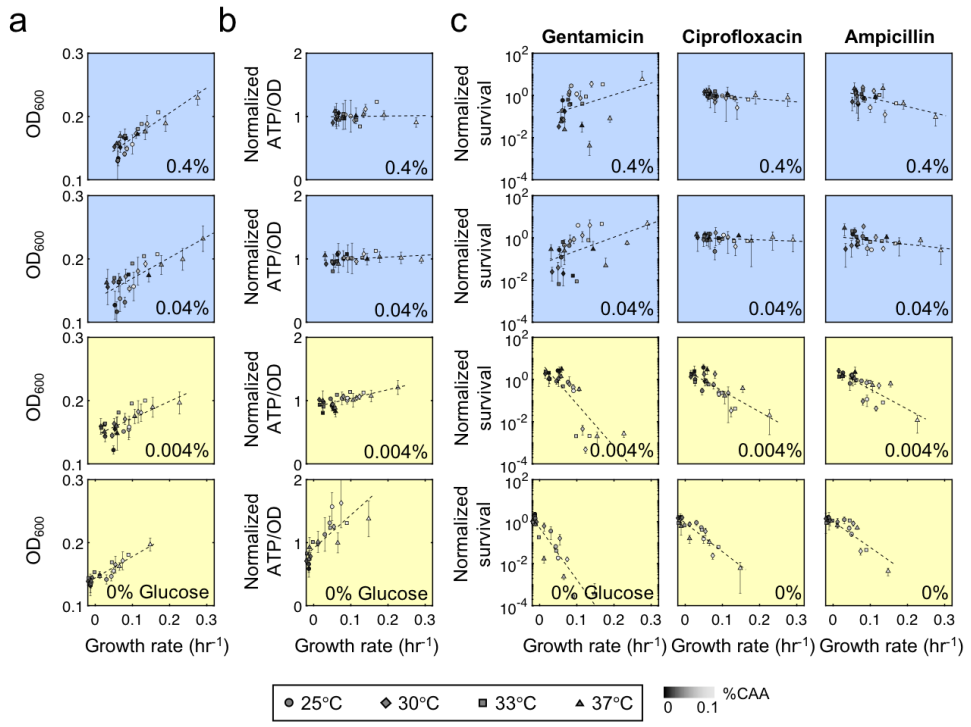

Supplementary Figure 6. Survival as a function of growth rate for normalized conditions

a. Temperature increases the range of overlapping cell densities across glucose concentrations. All parameters described in Fig. 1 (0, 0.004, 0.04, or 0.4% w/v glucose, 0, 0.001, 0.0025, 0.01, 0.025, or 0.1% w/v CAA, and 25, 30, 33, or 37°C) were combined and split into coupled and decoupled conditions (low and high glucose), indicated by box color (yellow or blue, respectively). Dark to light gray shading indicates increasing CAA, and markers (circle, diamond, square, and triangle) indicate increasing temperature, respectively. Conditions at different temperatures were normalized to the average spread to account for non-linear changes. Y-axis is OD_{600} and x-axis is growth rate. Growth rates are the mean of three biological replicates except for 33°C, which is two replicates. Error bars of the standard deviation are included when applicable.

b. Coupling and decoupling of metabolism and growth rate. Same conditions as described in (a). ATP/OD at different temperatures were normalized to the average ATP/OD per condition to account for non-linear changes. ATP/OD are the mean of three biological replicates except for 33°C, which is two replicates. Error bars of the standard deviation are included when applicable.

c. Lethality is correlated to growth rate only when growth and metabolism are coupled. The x-axis is growth rate and the y-axis is survival ratio normalized as described in Methods. Cells were treated with gentamicin, ciprofloxacin, and ampicillin for three hours at 20X MIC. The mean survival data is shown for four independent biological replicates on two individual days, except for 33°C which is two replicates. Light to dark shading indicates [CAA], and markers (circle, diamond, square, and triangle) indicate increasing temperature, respectively. Error bars of the standard deviation are included when applicable.

In all cases, single variable linear regression models are used to determine the correlation between growth rate and OD (a), ATP/OD (b), or survival (c), indicated by the dashed black lines. Statistical significance of each correlation can be found in Supplementary Table 5.

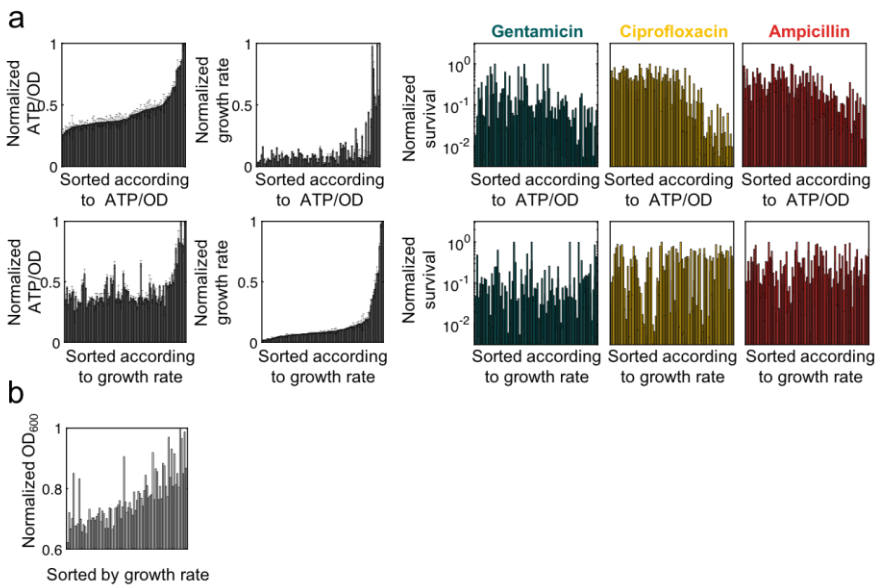

Supplementary Figure 7. Sorted ATP/OD and growth rate unaffected by data normalizations

a. Removing zero growth does not affect the overall trends. The trends are maintained when data from Fig. 4a are plotted without removing data points corresponding to zero measured growth. Thus, removing zero growth reduces likelihood of artifacts arising from low growth rate normalization.

b. Normalization validation. OD_{600} is taken as a control vector, as this correlates with growth rate under all conditions (Supplementary Fig. 6). Normalization process used in Fig. 4a does not disrupt this correlation.

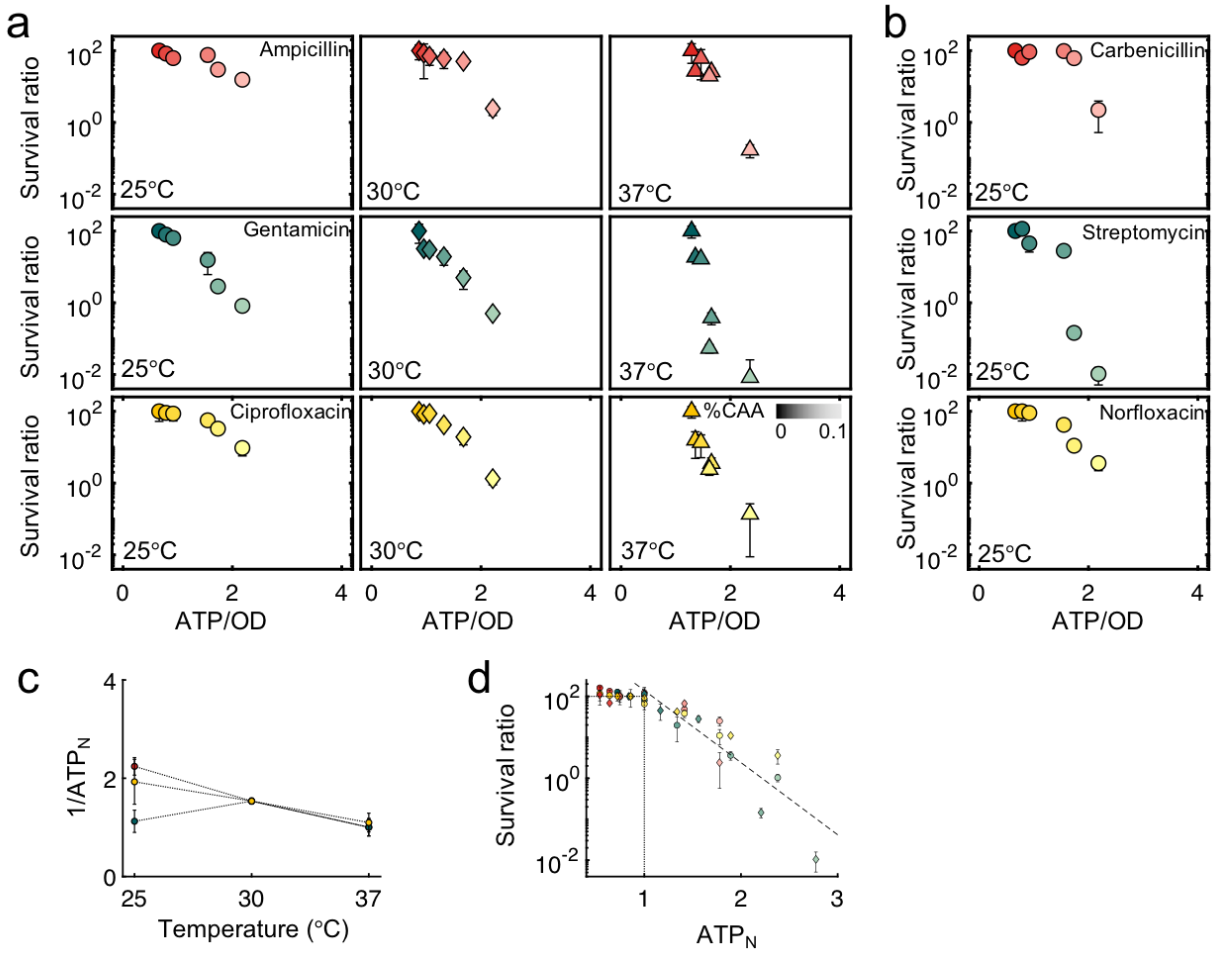

Supplementary Figure 8. Biphasic killing validation

a. Non-normalized survival exhibits biphasic trend. Survival in the absence of glucose for CAA at 0, 0.001, 0.0025, 0.01, 0.025, and 0.1% CAA exhibits biphasic dependence on intracellular ATP. The biphasic trend is most evident at low temperature, and appears to decrease as temperature increases (left to right). Colors green, gold, and red, indicate gentamicin, ciprofloxacin, and ampicillin, respectively. Drug concentration is 20X MIC.

b. Non-normalized survival exhibits biphasic trend for additional drugs. Carbenicillin (red), streptomycin (green), and norfloxacin (gold) show similar biphasic trends prior to normalization as those in (b) at 25°C. Concentrations used are 20X MIC.

c. ATP_N intuition. Intracellular ATP increases with increasing temperature. Thus, the difference between ATP_{crit} and the minimum ATP indicates the length of the plateau region on the biphasic curve. Intuitively, this region (defined by $1/ATP_N$) decreases with increasing temperature. In other words, the distance between ATP_{crit} and ATP_{min} is reduced. Solid line is shown as guide, not statistical fitting.

d. ATP_N trends are maintained for six bactericidal drugs. Data from (a) and (b) at 25°C. R^2=0.80. Correlation between ATP and survival is determined using single variable linear regression.

In all cases, data is the mean of four biological replicates on two independent days, and the error bar is the standard deviation.

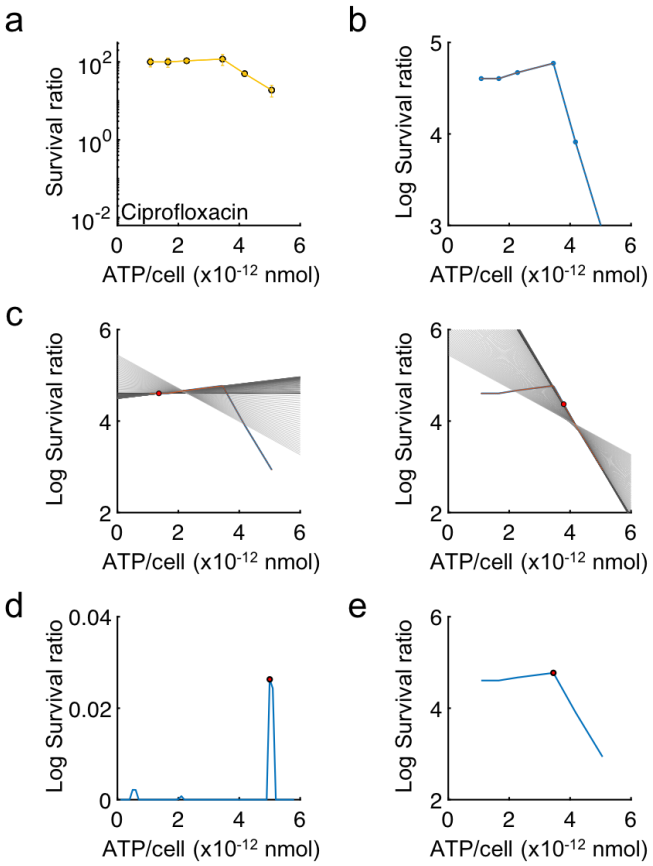

Supplementary Figure 9. Identifying the critical ATP threshold

a. Sample data. Ciprofloxacin at 2X MIC is shown for the data processing schematic (Fig. 4b).
b. Data interpolation. Data are first sorted along an increasing x-axis and the CFU is log-transformed. Linear interpolation is performed with 100-point mesh to account for CFU variability.
c. Linear fitting. First a line is fit in the forward direction (*left*), starting from the initial (lowest ATP_0) and extending point-wise. A line is then fit in the reverse direction (*right*) starting at the maximum ATP_0, and extending point-wise. The minimum and maximum slope in the forward and reverse direction, respectively, are taken as the best fits, and the corresponding index of each associated point is collected. We find the corresponding true data point closest to the collected interpolated point for each (i.e., non-interpolated). If the two true data points are the last and first points of the line, respectively, we use statistics to determine the output index, as this indicates the line is monotonic. Shaded lines from dark to light indicate best-fit lines from the first to the last point (e.g., shortest to longest line). Red circles indicate the index associated with the end point for the lines of best fit.
d. Identify inflection point to determine transition. If the lines are non-monotonic, the selected indices of the lines of best fit are used to define the region inside which we expect to find the maximal inflection point of the line. To ensure that the interpolated data we are searching contains all possible non-interpolated index candidates, we extend the region 17% in the outward direction, which ensures that we will not miss any non-interpolated points in the worst-case scenario. The second derivative is then used to find the maximum inflection point within the identified region.
e. Sample output. Red marker indicates critical ATP threshold.

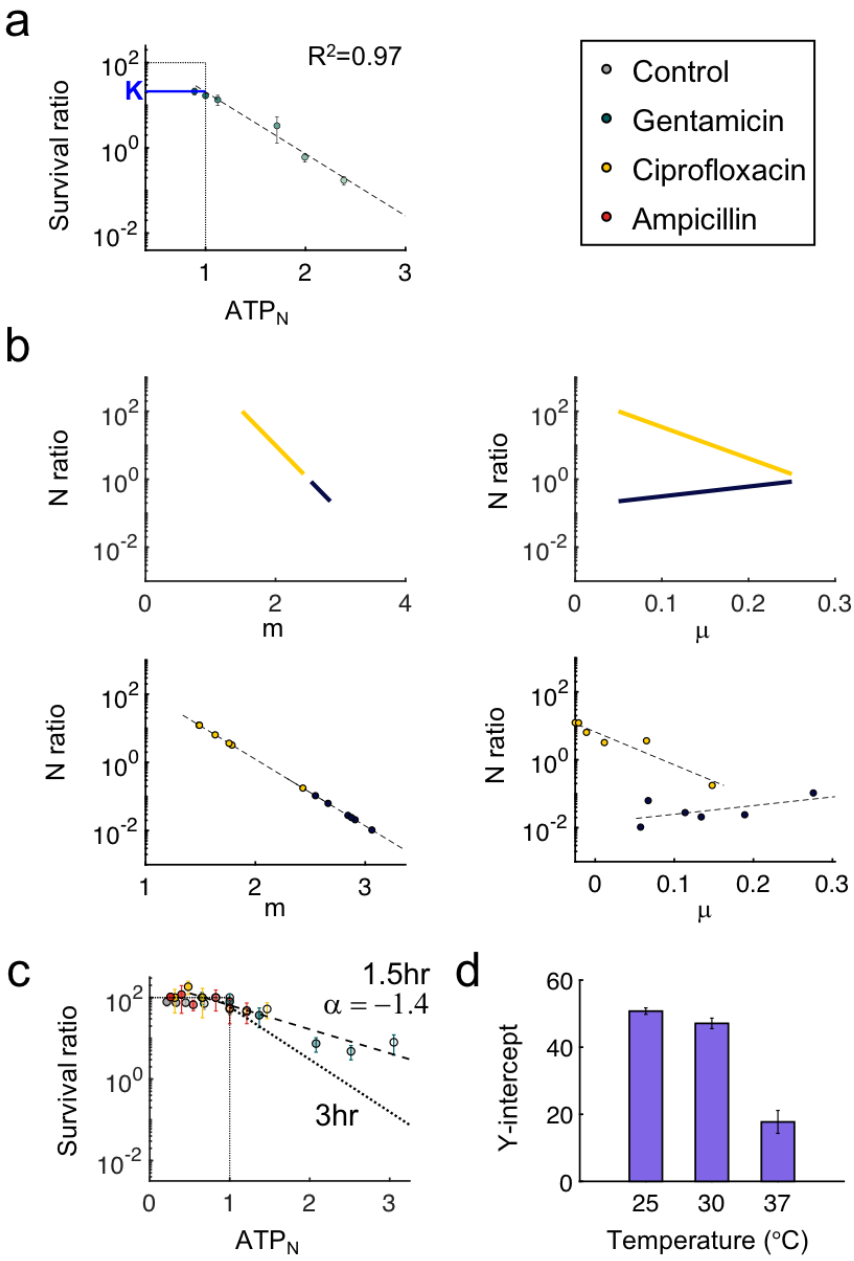

Supplementary Figure 10. Model validation and generality

a. Basal killing constant (K) depends on drug and other global variables. Example data set of gentamicin at 20X MIC is shown. K (in blue) represents the basal killing constant prior to the biphasic transition into log-linear metabolic-dependent killing; the blue line corresponds to the survival ratio at the minimum ATP. Same data as in Fig. 4b without normalization, which is the mean of four biological replicates; error bars are the standard deviation. Dashed line is the correlation between survival and ATP fit using a single variable linear regression model.

b. Model simulations validate experiments. Model is used to simulate conditions from Fig. 2 (parameters in Supplementary Table 6). Yellow indicates low glucose concentration (e.g., coupled), and blue indicates high glucose (e.g., decoupled). Survival is plotted either as a function of metabolism (m, left) or growth rate (μ, right). Growth rate and metabolism parameters were obtained from interpolating data at the extreme glucose concentrations (top row). This simplification does not change the conclusions, since the trend is maintained using discrete data points (bottom row). See Methods for model details. Dashed line indicates the single variable linear regression model fit.

c. Model validation: *Time-dependent slope*. Killing is quantified at 1.5 (circle markers), compared to three hours (dotted black line) following antibiotic addition. The slope of the linear region changes proportionally with time, consistent with mathematical interpretation. $R^2 = 0.83$ and α=-1.4. Dashed line is the single variable linear regression of survival as a function of ATP. Survival ratio is the mean of four biological replicates and error bars indicate standard deviation.

d. Model validation: *Basal survival decreases with increasing growth rate*. Data is from Fig. 4b. Error bars are the standard error associated with each intercept obtained from non-normalized linear regression fit.

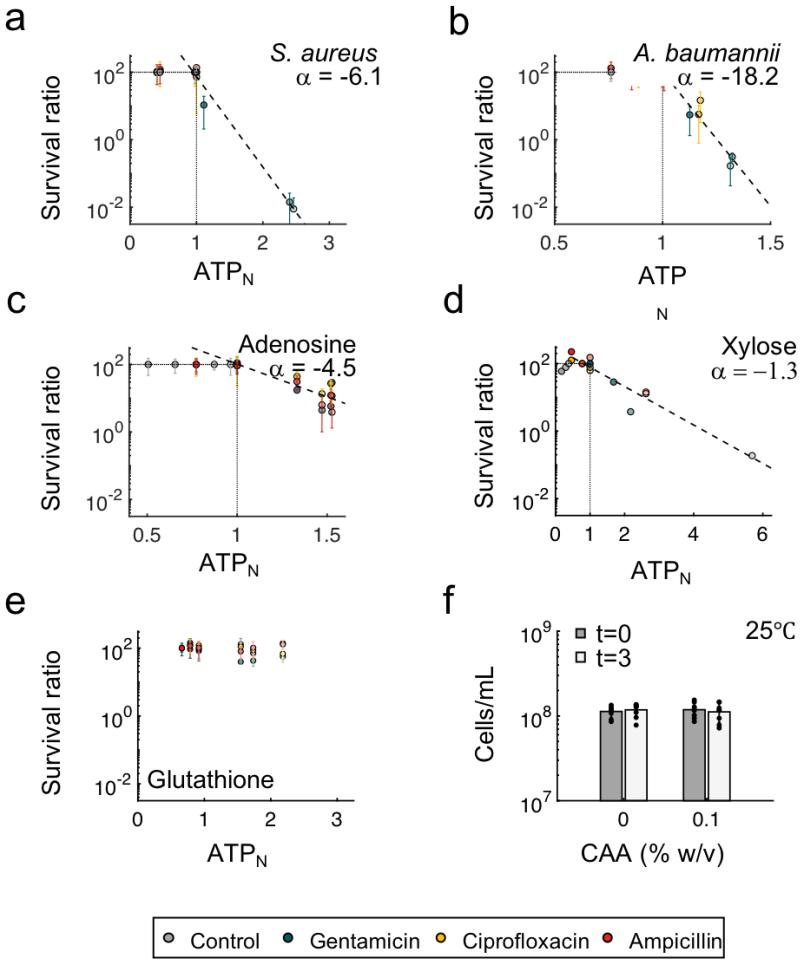

Supplementary Figure 11. CFU does not change significantly under additional diverse conditions

a-b. Results are general to Gram-positive and Gram-negative species. *Staphyloccus aureus* and *Acinetobacter baumannii* both exhibit metabolic-dependent killing with a critical ATP threshold at 25°C. CAA used is 0, 0.0025, 0.01, and 0.1% w/v. Data are the mean of three biological replicates and error bars show the standard deviation. Dashed line shows the linear regression of survival as a function of ATP.

c. Results are general to adenosine at concentrations of 0, 4, 12.6, 40, and 126.5 μg/mL at 25°C. Data are the average of three biological replicates and error bars show the standard deviation. Dashed line shows the linear regression of survival as a function of ATP.

d. Results are general to 0.04% w/v xylose as the sub-culture carbon source instead of glucose at 25°C. CAA is 0, 0.0025, 0.01, and 0.1% w/v. Data are the mean survival of two biological replicates. Dashed line is the single variable linear regression correlation.

e. Non-normalized glutathione data. Same data as in Fig. 4g, except without x-axis normalization. All antibiotics are used at 20X MIC; data are the mean survival of three biological replicates, and error bars are the standard deviations.

f. CFU changed insignificantly in the presence or absence of 0.1% CAA and 25°C over three hours. CFU was measured by spread plating 100 μL eight independent times to improve accuracy over spot plating; all replicates are shown in black.

E. coli strain BW25113 is used for all panels other than (a) and (b). In all panels except (f), shading (dark to light) indicates increasing CAA, and drug concentration is 20X MIC.

Supplementary Table 1. List of strains and species used in this study

List of strains and species used in this study, along with corresponding experiment.

Name	**Experiment/figure**	**Supplemented antibiotic**	**Source**
***Escherichia coli* strain BW25113**	All main figures and supplements	NA	Lab stock
Acinetobacter baumanii	Supplementary Fig. 11b	NA	Bringham and Women's Hospital; Strain #RB197
Staphylococcus aureus	Supplementary Fig. 11a	NA	Bringham and Women's Hospital; Strain #RB003
Δ*atpA*	Fig. 4f	Kanamycin	Keio Collection; JW3712-1

Supplementary Table 2. Metabolic network modeling parameters and outputs

a. Amino acid composition

	CAA (% w/v)					
Amino acid	**0**	**0.001**	**0.0025**	**0.01**	**0.025**	**0.1**
Ala (mM)	0.00E+00	3.37E-03	8.43E-03	3.37E-02	8.43E-02	3.37E-01
Arg (mM)	0.00E+00	1.38E-03	3.45E-03	1.38E-02	3.45E-02	1.38E-01
Asp (mM)	0.00E+00	5.26E-04	1.32E-03	5.26E-03	1.32E-02	5.26E-02
Cys (mM)	0.00E+00	8.26E-05	2.07E-04	8.26E-04	2.07E-03	8.26E-03
Glu (mM)	0.00E+00	1.03E-02	2.57E-02	1.03E-01	2.57E-01	1.03E+00
Gly (mM)	0.00E+00	1.87E-03	4.67E-03	1.87E-02	4.67E-02	1.87E-01
His (mM)	0.00E+00	1.29E-04	3.23E-04	1.29E-03	3.23E-03	1.29E-02
Ile (mM)	0.00E+00	2.37E-03	5.92E-03	2.37E-02	5.92E-02	2.37E-01
Leu (mM)	0.00E+00	3.51E-03	8.78E-03	3.51E-02	8.78E-02	3.51E-01
Lys (mM)	0.00E+00	1.44E-03	3.60E-03	1.44E-02	3.60E-02	1.44E-01
Met (mM)	0.00E+00	9.40E-04	2.35E-03	9.40E-03	2.35E-02	9.40E-02
Phe (mM)	0.00E+00	2.06E-03	5.15E-03	2.06E-02	5.15E-02	2.06E-01
Pro(mM)	0.00E+00	6.52E-03	1.63E-02	6.52E-02	1.63E-01	6.52E-01
Ser (mM)	0.00E+00	3.31E-04	8.26E-04	3.31E-03	8.26E-03	3.31E-02
Thr(mM)	0.00E+00	4.20E-04	1.05E-03	4.20E-03	1.05E-02	4.20E-02
Tyr (mM)	0.00E+00	2.21E-04	5.52E-04	2.21E-03	5.52E-03	2.21E-02
Val(mM)	0.00E+00	4.02E-03	1.00E-02	4.02E-02	1.00E-01	4.02E-01

b. Sugar composition

	Sugar % (w/v)						
Sugar	**0**	**0.002**	**0.004**	**0.008**	**0.04**	**0.08**	**0.4**
Glucose (mM)	0.000E+00	1.110E-01	2.220E-01	4.441E-01	2.220E+00	4.441E+00	2.220E+01
Xylose (mM)	0.000E+00	1.332E-01	2.664E-01	5.329E-01	2.664E+00	5.329E+00	2.664E+01
Maltose (mM)	0.000E+00	5.840E-02	1.169E-01	2.337E-01	1.169E+00	2.337E+00	1.169E+01

c. Biomass

		CAA (% w/v)					
		0.000	**0.001**	**0.0025**	**0.010**	**0.025**	**0.100**
Glucose (% w/v)	**0.000**	0.000	0.000	0.000	0.003	0.037	0.204
	0.002	0.000	0.000	0.002	0.019	0.053	0.220
	0.004	0.009	0.012	0.017	0.034	0.068	0.236
	0.008	0.031	0.035	0.040	0.062	0.097	0.266
	0.040	0.208	0.212	0.217	0.244	0.299	0.497
	0.080	0.429	0.433	0.438	0.465	0.520	0.769
	0.400	2.197	2.201	2.206	2.234	2.288	2.561
Xylose (% w/v)	**0.000**	0.000	0.000	0.000	0.003	0.037	0.204
	0.002	0.000	0.000	0.002	0.019	0.052	0.220
	0.004	0.009	0.012	0.016	0.034	0.068	0.235
	0.008	0.031	0.034	0.039	0.062	0.097	0.266
	0.040	0.205	0.209	0.214	0.242	0.296	0.493

	0.080	0.423	0.427	0.433	0.460	0.514	0.762
	0.400	2.169	2.173	2.179	2.206	2.261	2.534
Maltose (% w/v)	**0.000**	0.000	0.000	0.000	0.003	0.037	0.204
	0.002	0.000	0.000	0.003	0.020	0.053	0.221
	0.004	0.010	0.014	0.018	0.036	0.070	0.237
	0.008	0.033	0.037	0.042	0.065	0.100	0.270
	0.040	0.220	0.223	0.229	0.256	0.310	0.511
	0.080	0.452	0.456	0.461	0.489	0.543	0.797
	0.400	2.313	2.317	2.323	2.350	2.405	2.678

d. ATP production normalized by biomass

		CAA (% w/v)					
		0.000	**0.001**	**0.0025**	**0.010**	**0.025**	**0.100**
Glucose (% w/v)	**0.000**	0.000	0.000	0.000	972.378	134.067	72.857
	0.002	0.000	0.000	1198.055	196.523	108.788	70.861
	0.004	347.839	262.664	207.890	131.990	95.604	69.324
	0.008	135.734	127.042	117.135	94.816	81.579	67.145
	0.040	66.370	66.041	65.567	63.591	61.048	58.799
	0.080	60.126	60.018	59.859	59.119	58.014	55.778
	0.400	55.399	55.385	55.365	55.266	55.075	54.292
Xylose (% w/v)	**0.000**	0.000	0.000	0.000	972.378	134.067	72.857
	0.002	0.000	0.000	1309.277	197.737	108.898	70.949
	0.004	356.369	266.686	210.483	132.573	95.695	69.308
	0.008	136.557	127.634	117.507	94.944	81.596	67.109
	0.040	65.884	65.559	65.092	63.150	60.665	58.632
	0.080	59.574	59.469	59.314	58.598	57.540	55.529
	0.400	54.799	54.786	54.768	54.675	54.496	53.770
Maltose (% w/v)	**0.000**	0.000	0.000	0.000	972.378	134.067	72.857
	0.002	0.000	0.000	889.274	190.598	107.905	70.764
	0.004	313.123	244.425	195.671	128.408	94.571	69.196
	0.008	129.843	122.273	113.504	92.884	80.579	66.945
	0.040	65.728	65.426	64.992	63.151	60.781	58.550
	0.080	59.824	59.724	59.576	58.887	57.838	55.590
	0.400	55.341	55.328	55.309	55.216	55.035	54.276

e. Compiled nitrogen to carbon (N:C) ratio

CAA (% w/v)	**Sugar (% w/v)**	**N:C**
0.0025	0.4	0.0062
0.0025	0.08	0.0312
0.0025	0.04	0.0625
0.01	0.08	0.125
0.01	0.04	0.25
0.01	0.008	1.25
0.1	0.04	2.5
0.1	0.008	12.5
0.1	0.004	25

Supplementary Table 3. Regression statistics for decoupled growth and metabolism.
Data was collected in biological triplicate for all conditions except 33°C, which is two replicates.

a. Multi-variable linear regression model with no interactions for growth rate.

	Estimate	SE	t-statistic	p-value	F-stat	R^2
Intercept	-0.10	0.03	-3.00	0.004	28.1	0.50
CAA	0.91	0.12	7.44	1.1e-10		
Glucose	0.77	0.03	2.96	0.004		
Temperature	0.0049	0.001	4.75	9.1e-6		

b. Multi-variable linear regression model with no interactions for metabolism.

	Estimate	SE	t-statistic	p-value	F-stat	R^2
Intercept	0.780	0.36	2.19	0.03	13	0.27
CAA	3.72	1.38	2.69	0.008		
Glucose	1.38	0.29	4.73	8.0e-6		
Temperature	0.034	0.011	2.04	0.003		

c. Single-variable linear regression for growth rate as a function of CAA. Linear regression models are fit to the six growth rate data points at each CAA concentration. Tests for all t-statistics are two-sided. Green highlighted rows indicate the particular condition met decoupling requirements.

Temperature (°C)	Glucose	p-value	Intercept estimate	Slope estimate	R^2	SSE
25	0	0.0021	0.0729	0.0095	0.9265	0.0013
30	0	0.0156	0.0957	0.0133	0.8033	0.0033
33	0	0.0286	0.1026	0.0146	0.7369	0.0044
37	0	0.0269	0.1687	0.0247	0.7447	0.0072
25	0.004	0.0146	0.1252	0.0120	0.8095	0.0029
30	0.004	0.0117	0.1710	0.0190	0.8284	0.0043
33	0.004	0.0018	0.1789	0.0229	0.9317	0.0031
37	0.004	0.0039	0.2889	0.0356	0.9003	0.0059
25	0.04	0.0128	0.1218	0.0090	0.8214	0.0021
30	0.04	0.0113	0.1719	0.0178	0.8316	0.0040
33	0.04	0.0301	0.1958	0.0185	0.7306	0.0056
37	0.04	0.0329	0.3736	0.0419	0.7192	0.0131
25	0.4	0.0018	0.1150	0.0078	0.9316	0.0011
30	0.4	0.0074	0.1650	0.0154	0.8631	0.0031
33	0.4	0.0038	0.1971	0.0172	0.9008	0.0029
37	0.4	0.0195	0.3276	0.0364	0.7811	0.0096

d. Single-variable linear regression for ATP/OD as a function of CAA. Linear regression models are fit to the six ATP/OD data points at each CAA concentration. Tests for all t-statistics are two-sided. Green highlighted rows indicate the particular condition met decoupling requirements.

e.

Temperature (°C)	Glucose	P-value	Intercept estimate	Slope estimate	R^2	SSE
25	0	0.0001	2.8410	0.2784	0.9839	0.0178
30	0	0.0009	2.6014	0.2465	0.9515	0.0278
33	0	0.0042	2.4267	0.1686	0.8966	0.0286
37	0	0.0142	2.5846	0.1586	0.8117	0.0382
25	0.004	0.0841	2.2693	0.0365	0.5667	0.0159
30	0.004	0.0680	1.9468	0.0506	0.6065	0.0204
33	0.004	0.0087	2.4395	0.1167	0.8515	0.0244
37	0.004	0.0167	2.9140	0.1337	0.7964	0.0338
25	0.04	0.2292	2.4600	0.0373	0.3345	0.0263
30	0.04	0.6255	2.3621	0.0195	0.0651	0.0369
33	0.04	0.4276	3.1107	0.0626	0.1628	0.0710
37	0.04	0.9457	3.1866	-0.0052	0.0013	0.0718
25	0.4	0.2656	2.4152	0.0205	0.2948	0.0159
30	0.4	0.4856	2.4892	0.0325	0.1284	0.0423
33	0.4	0.4523	2.6250	0.0581	0.1475	0.0698

37	0.4	0.2664	2.5576	-0.0500	0.2940	0.0387

f. Regression for normalized dataset from Fig. 4a.

	p-value	Intercept estimate	Slope estimate	R^2	SSE
Normalized Growth	<0.001	0.53	0.40	0.116	0.011
Normalized ATP	0.999	0.43	-1.48×10^{-5}	3.39×10^{-8}	0.0095

Supplementary Table 4. MICs for all strains/drugs used in this study

Comprehensive list of strains and species used in this study and their associated MIC values. Measurements were performed in biological triplicate, and the range is reported along with the concentration used to determine 2X and 20X.

a. MIC range and values for main strain BW25113

Drug	MIC range (μg/mL)	MIC used (μg/mL)
Ampicillin	[6.0-10.0]	10.0
Gentamicin	[0.25-0.5]	.25
Ciprofloxacin	[0.025-0.05]	0.05
Streptomycin	[2.5-10.0]	2.5
Norfloxacin	[0.25-0.65]	0.5
Cefsulodin	[8.0-16.0]	16.0
Carbenicillin	[6.0-10.0]	10
Kanamycin	[2.5-5.0]	2.5
Levofloxacin	0.5	0.5

b. MIC values for additional strains/species in μg/mL

Drug	***S. aureus***	***A. baumanii***	**Δ*atpA***
Ampicillin	16.0	16.0	10.0
Gentamicin	5.0	2.5	1.0
Ciprofloxacin	0.8	0.8	0.05

c. 95% confidence intervals for Fig. 2c

	Survival by ATP/OD	Survival by growth rate	
% Glucose:	0.004% and 0.04% combined	0.004%	0.04%
Kanamycin	-8.78:-3.29	-41.08:-8.61	9.53:26.55
Streptomycin	-7.02:-1.47	-41.13:-1	12.53:25.76
Gentamicin	-9.69:-4.56	-65.63:-13.68	-9.27:25.75
Levofloxacin	-4.48:-2.11	-28.88:-3.34	-0.24:11.14
Norfloxacin	-3.47:-1.34	-22.09:-2.05	-3.68:4.76
Ciprofloxacin	-4.36:-1.67	-36.17:-7.48	-4.66:2.44
Cefsulodin	-3.11:-1.06	-14.5:-4.56	-0.24:10.9
Carbenicillin	-5.5:-0.99	-28.03:-4.8	-0.54:26.17
Ampicillin	-6.52:-2.78	-38.77:-6.88	-14.14:2.21

Supplementary Table 5. Statistical testing for survival by growth or ATP/OD in Fig. 3
All survival data from Fig. 2 and 3 was measured in four biological replicates, except for 33°C which is two biological replicates. Linear regression models were individually fit for each glucose and temperature combination as a function of the six CAA concentrations. Results from statistical testing are split into individual sub-tables:

a. 95% confidence intervals

Bold font is for conditions where the confidence interval indicated insignificant or significant slopes for coupled and uncoupled conditions, respectively. Yellow color highlights conditions verified as a statistical outlier based on the overall error of associated CFU measurements. See Methods for details.

		Survival by ATP/OD (Fig. 3b)						Survival by growth rate (Fig. 3a)			
% Glucose		0%	0.004%	0.04%	0.4%	% Glucose		0%	0.004%	0.04%	0.4%
Gent	25°C	-4.27:-2.72	-12.7:-0.45	-8.72:15.05	-17.27:28.63	Gent	25°C	-89.55:-37.05	**-48.23:6.28**	17.7:89.22	-12.45:135.28
	30°C	-4.6:-2.66	-47.7:14.04	-15.02:24.64	-5.99:17.2		30°C	-64.45:-23.69	-130.93:-25.37	25.37:84.26	10.13:85.56
	33°C	-14.22:-3.78	-21.4:-0.53	-5.9:15.41	-1.19:4.79		33°C	-94.02:-52.26	-97.71:-36.73	-23.34:110.06	4.44:36.34
	37°C	-16.62:-1.76	-17.13:-1.86	-17.17:12.48	-22.48:6.56		37°C	-80.31:-22.03	-65.53:-13.56	-9.27:25.71	-5.57:49.2
Cipro	25°C	-2.27:-0.76	-17.34:-3.18	-7.2:8.18	-3.5:4.42	Cipro	25°C	-46.59:-5.91	**-71.12:21.35**	-54.77:44.56	-22.72:10.53
	30°C	-4.3:-2.04	-20.25:10.88	-5.39:2.8	-6.99:2.82		30°C	-60.06:-15.72	**-62.34:3.05**	-21.25:9.92	**-35.06:-3.75**
	33°C	-5.63:-0.69	-9.65:-0.12	-1.69:0.5	-1.55:0.98		33°C	-38.44:-14.3	-42.84:-18.14	**-10.91:-1.61**	-13.15:0.7
	37°C	-8.94:-3.02	-9.43:-1.02	-1.49:3.44	-0.55:2.69		37°C	-46.64:-15.52	-36.11:-7.42	-4.66:2.44	-6.02:2.58
Amp	25°C	-1.94:-0.37	-17.81:3.46	-11.05:4.82	-14.73:8.25	Amp	25°C	-38.88:-0.27	**-64.04:8.94**	**-64.77:-10.21**	**-52.08:-28.89**
	30°C	-4.2:-0.78	-21.82:7.08	-8.64:8.7	-10.19:2.54		30°C	-56.46:-0.68	**-66.6:8.11**	-28.69:37.78	-54.14:30.31
	33°C	-6.43:1.3	-7.49:1.93	-2.36:-0.53	-2.77:0.97		33°C	-46.34:-2.17	-35.75:-5.6	**-17.81:-1.84**	-22.53:2.24
	37°C	-8.9:-3.59	-10:-1.03	-2.99:10.41	1.43:9.9		37°C	-48.93:-14.31	-38.69:-6.85	-14.13:2.21	-23.91:1.95

b. P-values

		Survival by ATP/OD (Fig. 3b)						Survival by growth rate (Fig. 3a)			
% Glucose		0%	0.004%	0.04%	0.4%	% Glucose		0%	0.004%	0.04%	0.4%
Gent	25°C	0.0002	0.0005	0.0087	0.0265	Gent	25°C	0.0026	0.0039	0.0006	0.0082
	30°C	0.0051	0.0015	0.0236	0.005		30°C	0.0231	0.009	0.0037	0.0052
	33°C	0.0148	0.0156	0.1389	0.0028		33°C	0.048	0.0467	0.038	0.0071
	37°C	0.0407	0.2047	0.0433	0.0259		37°C	0.0994	0.0147	0.0036	0.0134
Cipro	25°C	0.0158	0.4505	0.0465	0.026	Cipro	25°C	0.2094	0.0655	0.0024	0.0136
	30°C	0.1344	0.2298	0.176	0.0269		30°C	0.1041	0.0954	0.019	0.0165
	33°C	0.5002	0.5375	0.2831	0.6832		33°C	0.0143	0.0067	0.1454	0.2618
	37°C	0.8679	0.4296	0.2049	0.3352		37°C	0.7895	0.3701	0.0202	0.4348
Amp	25°C	0.3368	0.9926	0.0116	0.1987	Amp	25°C	0.0189	0.7235	0.0269	0.1129
	30°C	0.5298	0.2509	0.1705	0.2028		30°C	0.0822	0.0244	0.0238	0.0914
	33°C	0.7613	0.3036	0.5683	0.14		33°C	0.3663	0.0263	0.0671	0.3294
	37°C	0.4776	0.1703	0.2537	0.0206		37°C	0.0006	0.4772	0.0854	0.0779

c. R^2

		Survival by ATP/OD (Fig. 3b)						Survival by growth rate (Fig. 3a)			
% Glucose		0%	0.004%	0.04%	0.4%	% Glucose		0%	0.004%	0.04%	0.4%

Gent	25°C	0.97	0.96	0.85	0.75	Gent	25°C	0.92	0.90	0.96	0.86
	30°C	0.89	0.94	0.76	0.89		30°C	0.76	0.85	0.90	0.88
	33°C	0.81	0.80	0.46	0.91		33°C	0.66	0.67	0.70	0.87
	37°C	0.69	0.36	0.68	0.75		37°C	0.53	0.81	0.90	0.82
Cipro	25°C	0.8	0.15	0.67	0.75	Cipro	25°C	0.36	0.61	0.92	0.82
	30°C	0.47	0.33	0.40	0.74		30°C	0.52	0.54	0.78	0.80
	33°C	0.12	0.10	0.28	0.05		33°C	0.81	0.87	0.45	0.30
	37°C	0.01	0.16	0.36	0.23		37°C	0.02	0.20	0.78	0.16
Amp	25°C	0.23	0.00	0.83	0.37	Amp	25°C	0.78	0.03	0.74	0.51
	30°C	0.11	0.31	0.41	0.37		30°C	0.57	0.76	0.76	0.55
	33°C	0.03	0.26	0.09	0.46		33°C	0.21	0.75	0.61	0.24
	37°C	0.13	0.41	0.31	0.78		37°C	0.96	0.13	0.56	0.58

d. Slope estimate

		Survival by ATP/OD (Fig. 3b)						Survival by growth rate (Fig. 3a)			
% Glucose		0%	0.004%	0.04%	0.4%	% Glucose		0%	0.004%	0.04%	0.4%
Gent	25°C	-3.50	-3.63	-9.00	-9.19	Gent	25°C	-63.3	-44.07	-73.14	-51.17
	30°C	-1.52	-3.17	-3.16	-5.98		30°C	-26.25	-37.89	-26.37	-31.08
	33°C	-1.16	-2.49	-2.57	-6.25		33°C	-19.58	-28.57	-24.25	-31.62
	37°C	-6.58	-16.83	-10.96	-9.5		37°C	-20.97	-78.15	-67.22	-39.55
Cipro	25°C	-10.26	-4.68	-4.89	-5.23	Cipro	25°C	-24.89	-29.65	-30.49	-21.77
	30°C	-7.17	-7.37	-2.78	-5.52		30°C	-27.55	-29.24	-20.67	-22.77
	33°C	3.17	4.81	4.75	-2.35		33°C	53.46	54.82	43.36	8.22
	37°C	0.49	-1.30	-0.60	0.97		37°C	-5.11	-5.66	-6.26	-1.11
Amp	25°C	-3.12	0.03	-1.45	3.71	Amp	25°C	-37.49	4.54	-9.83	-5.96
	30°C	5.68	5.6	1.80	-7.96		30°C	61.42	47.85	20.39	21.82
	33°C	0.46	-2.08	-0.28	1.07		33°C	-6.09	-19.40	-6.22	-1.72
	37°C	-3.24	-3.83	-0.90	5.67		37°C	-40.48	-11.91	-10.14	-10.98

e. Supplementary Fig. 6 linear regression statistical significance

	% Glucose (w/v):	**0**	**0.004**	**0.04**	**0.4**
P-value	**Gent**	0.0082	0.0052	0.0071	0.0134
	Cipro	0.0136	0.0165	0.2618	0.4348
	Amp	0.1129	0.0914	0.3294	0.0779

	% Glucose (w/v):	**0**	**0.004**	**0.04**	**0.4**
Slope estimate	**Gent**	-51.17	-31.08	-31.62	-39.55
	Cipro	-21.77	-22.77	8.22	-1.11
	Amp	-5.96	21.82	-1.72	-10.98

	% Glucose (w/v):	**0**	**0.004**	**0.04**	**0.4**
R^2	**Gent**	0.86	0.88	0.87	0.82
	Cipro	0.82	0.80	0.30	0.16
	Amp	0.51	0.55	0.24	0.58

	% Glucose (w/v):	**0**	**0.004**	**0.04**	**0.4**
95% CI	**Gent**	-80.31:-22.03	-65.53:-13.56	-9.27:25.71	-5.57:49.2
	Cipro	-46.64:-15.52	-36.11:-7.42	-4.66:2.44	-6.02:2.58
	Amp	-48.93:-14.31	-38.69:-6.85	-14.13:2.21	-23.91:1.95

f. Standard deviation of survival data

Yellow highlight indicates those conditions where the spread in survival was greater than the average error associated with the CFU measurements. For each temperature/glucose condition the standard deviation accounts for the spread in all six data points at every CAA concentration.

		Standard deviation of Survival by ATP/OD (Fig. 3b)			
% Glucose		**0%**	**0.004%**	**0.04%**	**0.4%**
Gent	25°C	9.0500	82.9000	8.8600	21.3400
	30°C	13.9000	23.6900	0.0200	0.1900
	33°C	35.2100	36.2600	0.0400	0.0500
	37°C	86.4500	33.9500	0.0500	2.4600
Cipro	25°C	20.8000	2.1000	0.1000	0.0700
	30°C	25.8200	7.2400	0.1600	0.2900
	33°C	16.1100	22.0100	0.3900	0.4000
	37°C	68.3600	11.8200	0.1100	0.0800
Amp	25°C	25.9100	21.0200	6.2800	4.8300
	30°C	28.2300	22.0800	6.9400	3.7400
	33°C	38.5400	34.7800	2.3600	2.4100
	37°C	40.2000	21.3700	0.2300	0.3500

Supplementary Table 6: Comparison of ATP_{crit}

a. Raw ATP_{crit}

	Control (min)	Control (max)	Gentamicin (20X)	Ciprofloxacin (20X)	Ampicillin (20X)
Adenosine	0.19	0.24	0.24	0.24	0.19
Malic acid	0.13	0.13	0.33	0.33	0.13
A. baumanii	0.80	0.90	1.05	1.05	0.80
S. aureus	0.39	0.95	0.95	0.95	0.39
25°C	0.82	0.92	1.84	1.84	0.82
30°C	0.85	1.31	1.31	1.31	0.85
37°C	1.49	1.49	1.63	1.49	1.49
Δ*atpA*	1.59	1.59	2.11	2.12	1.59
Glutathione	0.23	0.51	0.54	0.54	0.23

b. ATP_{crit} adjusted by the initial metabolic state for that condition

	Control (min)	Gentamicin (20X)	Ciprofloxacin (20X)	Ampicillin (20X)
Adenosine	1.00	1.29	1.29	1.29
Malic acid	1.00	0.99	2.48	2.48
A. baumanii	1.00	1.13	1.31	1.31
S. aureus	1.00	2.46	2.46	2.46
25°C	1.00	1.12	2.24	2.24
30°C	1.00	1.54	1.54	1.54
37°C	1.00	1.00	1.10	1.00
Δ*atpA*	1.00	1.00	1.33	1.34
Glutathione	1.00	2.28	2.37	2.37

c. Adjusted ATP_{crit} normalized by ATP_{crit} at 25°C to compare average values. The slope overall increases with decreasing ATP_{crit}.

	Control (min)	ATP_{crit} for Gentamicin (20X)	ATP_{crit} for Ciprofloxacin (20X)	ATP_{crit} for Ampicillin (20X)	Average ATP_{crit}	Slope (α)
Adenosine	1.00	1.15	0.58	0.58	0.77	-4.5
Malic acid	1.00	0.88	1.11	1.11	1.03	-3.3
A. baumanii	1.00	1.00	0.59	0.59	0.72	-6.1
S. aureus	1.00	2.19	1.10	1.10	1.46	-2.0
25°C	1.00	1.00	1.00	1.00	1.00	-3.0
30°C	1.00	1.37	0.68	0.68	0.91	-5.4
37°C	1.00	0.89	0.49	0.45	0.61	-10.4
Δ*atpA*	1.00	0.89	0.59	0.60	0.69	-14.6
Glutathione	1.00	2.02	1.06	1.06	1.38	-1.2

Supplementary Table 7. Model parameters

Parameter	Name	Low glucose	High glucose	Description
μ	Growth rate (hr^{-1})	[0.001-0.025]	[0.05-0.25]	Obtained from main dataset (Fig. 1c).
m	ATP (μM/OD)	[1.07-2.63]	[3.11-2.56]	Obtained from main dataset (Fig. 1c).
d	Antibiotic death rate (hr^{-1})	1.5	1.5	Fitted from Fig. 4b
t	Time (hr)	3	3	Consistent with experimental conditions
A	Antibiotic (A.U.)	1	1	Unitless drug concentration
N_0	Initial cell density (OD)	[0.14-0.20]	[0.18-0.24]	Determined by OD ranges

Supplementary Table 8. Comparisons of slopes

A comparison of all quantified slopes from main and supplemental experiments at 20X MIC.

Perturbation	Condition (figure)	[Drug]	[Metabolite]	Slope	Normalized slope*	R^2	# replicates
Metabolite	Casamino acid (4b)	20X	0, 0.001, 0.0025, 0.01, 0.025, 0.1 % w/v	-3.0	-1.0	0.98	4
	Malic acid (4e)	20X	0, 4, 12.6, 40, 126.5 μg/mL	-3.3	-1.4	0.94	4
	Adenosine (S11c)	20X	0, 4, 12.6, 40, 126.5 μg/mL	-4.5	-1.6	0.82	3
	Glutathione (4g)	20X	0, 0.0025, 0.01, 0.1 % w/v	-1.2	-0.4	0.42	3
Pre-growth carbon source	Xylose (S11d)	20X	0, 0.0025, 0.01, 0.1 % w/v	-1.3	-0.4	0.91	2
Time	1.5hr (S10c)	20X	0, 0.001, 0.0025, 0.01, 0.025, 0.1 % w/v	-1.4	-0.9	0.83	4
	3hr (4b)	20X	0, 0.001, 0.0025, 0.01, 0.025, 0.1% w/v	-2.96	-1.2	0.98	4
Strains/species	*S. aureus* (S11a)	20X	0, 0.0025, 0.01, 0.1 % w/v	-6.1	-2.0	0.98	3
	A. baumannii (S11b)	20X	0, 0.0025, 0.01, 0.1 % w/v	-18.2	-6.1	0.95	3
	Δ*atpA* (4f)	20X	0, 0.01, 0.1 % w/v	-14.6	-4.9	0.96	3
Temperature	25°C (4b)	20X	0, 0.001, 0.0025, 0.01, 0.025, 0.1 % w/v	-3.0	-1.0	0.70	4
	30°C (4b)	20X	0, 0.001, 0.0025, 0.01, 0.025, 0.1 % w/v	-5.4	-1.7	0.85	4
	37°C (4b)	20X	0, 0.001, 0.0025, 0.01, 0.025, 0.1 % w/v	-10.4	-2.8	0.85	4

* Indicates normalized by time

References

1. Zampieri, M., Zimmermann, M., Claassen, M. & Sauer, U. Nontargeted Metabolomics Reveals the Multilevel Response to Antibiotic Perturbations. *Cell Rep.* **19,** 1214–1228 (2017).
2. Høiby, N., Bjarnsholt, T., Givskov, M., Molin, S. & Ciofu, O. Antibiotic resistance of bacterial biofilms. *Int. J. Antimicrob. Agents* **35,** 322–332 (2010).
3. Yang, J. H., Bening, S. C. & Collins, J. J. Antibiotic efficacy — context matters. *Curr. Opin. Microbiol.* **39,** 73–80 (2017).
4. Lee, A. J. *et al.* Robust, linear correlations between growth rates and β-lactam-mediated lysis rates. *Proc. Natl. Acad. Sci. U. S. A.* **115,** 4069–4074 (2018).
5. Eng, R. H., Padberg, F. T., Smith, S. M., Tan, E. N. & Cherubin, C. E. Bactericidal effects of antibiotics on slowly growing and nongrowing bacteria. *Antimicrob. Agents Chemother.* **35,** 1824–8 (1991).
6. Dwyer, D. J., Collins, J. J. & Walker, G. C. Unraveling the Physiological Complexities of Antibiotic Lethality. *Annu. Rev. Pharmacol. Toxicol.* **55,** 313–332 (2015).
7. Lobritz, M. A. *et al.* Antibiotic efficacy is linked to bacterial cellular respiration. *Proc. Natl. Acad. Sci.* **112,** 8173–8180 (2015).
8. Meylan, S. *et al.* Carbon Sources Tune Antibiotic Susceptibility in Pseudomonas aeruginosa via Tricarboxylic Acid Cycle Control. *Cell Chem. Biol.* **24,** 195–206 (2017).
9. Allison, K. R., Brynildsen, M. P. & Collins, J. J. Metabolite-enabled eradication of bacterial persisters by aminoglycosides. *Nature* **473,** 216–220 (2011).
10. Li, J. *et al.* Antimicrobial Activity and Resistance: Influencing Factors. *Front. Pharmacol.* **8,** 364 (2017).
11. Meylan, S., Andrews, I. W. & Collins, J. J. Targeting Antibiotic Tolerance, Pathogen by Pathogen. *Cell* **172,** 1228–1238 (2018).
12. Brauner, A., Fridman, O., Gefen, O. & Balaban, N. Q. Distinguishing between resistance, tolerance and persistence to antibiotic treatment. *Nat. Rev. Microbiol.* **14,** 320–330 (2016).
13. Knudsen, G. M., Ng, Y. & Gram, L. Survival of Bactericidal Antibiotic Treatment by a Persister Subpopulation of Listeria monocytogenes. *Appl. Environ. Microbiol.* **79,** 7390–7397 (2013).
14. Molenaar, D., van Berlo, R., de Ridder, D. & Teusink, B. Shifts in growth strategies reflect tradeoffs in cellular economics. *Mol. Syst. Biol.* **5,** 323 (2009).
15. Qusheng, J. & Bethke, C. M. The thermodynamics and kinetics of microbial metabolism. (2007). doi:10.2475/04.2007.01
16. Lele, U. N. & Watve, M. G. Bacterial Growth Rate and Growth Yield: Is There A Relationship? *Proc Indian Natn Sci Acad* **80,** 537–546 (2014).
17. Lipson, D. A. The complex relationship between microbial growth rate and yield and its implications for ecosystem processes. *Front. Microbiol.* **6,** 615 (2015).
18. Kayser, A. *et al.* Metabolic flux analysis of Escherichia coli in glucose-limited continuous culture. I. Growth-rate-dependent metabolic efficiency at steady state. doi:10.1099/mic.0.27481-0
19. Szenk, M., Dill, K. A. & De Graff, A. M. R. Why Do Fast-Growing Bacteria Enter Overflow Metabolism? Testing the Membrane Real Estate Hypothesis. *Cell Syst.* (2017). doi:10.1016/j.cels.2017.06.005
20. Basan, M. *et al.* Overflow metabolism in Escherichia coli results from efficient proteome allocation. *Nature* **528,** 99–104 (2015).
21. Russell, J. B. & Cook, G. M. *Energetics of Bacterial Growth: Balance of Anabolic and Catabolic Reactions. MICROBIOLOGICAL REVIEWS* **59,** (1995).
22. Low, E. W. & Chase, H. A. Reducing production of excess biomass during wastewater treatment. *Water Res.* **33,** 1119–1132 (1999).
23. Chudoba, P., Morel, A. & Capdeville, B. The case of both energetic uncoupling and metabolic selection of microorganisms in the OSA activated sludge system. *Environ. Technol.* **13,** 761–770 (1992).
24. Liu, Y. Energy uncoupling in microbial growth under substrate-sufficient conditions. *Appl. Microbiol. Biotechnol.* **49,** 500–505 (1998).
25. Waschina, S., Souza, G. D', Kost, C. & Kaleta, C. Metabolic network architecture and carbon source determine metabolite production costs. *FEBS J.* 2149–2163 (2016). doi:10.1111/febs.13727
26. Akashi, H. & Gojobori, T. Metabolic efficiency and amino acid composition in the proteomes of Escherichia coli and Bacillus subtilis. *Proc. Natl. Acad. Sci. U. S. A.* **99,** 3695–700 (2002).
27. Akashi, H. & Gojobori, T. Metabolic efficiency and amino acid composition in the proteomes of Escherichia coli and Bacillus subtilis. *Proc. Natl. Acad. Sci. U. S. A.* **99,** 3695–700 (2002).
28. Gschaedler, A. & Boudrant, J. Amino acid utilization during batch and continuous cultures of Escherichia coli on a semi-synthetic medium. *J. Biotechnol.* **37,** 235–251 (1994).
29. Andersent, K. B. & Von Meyenburgt, K. *Are Growth Rates of Escherichia coli in Batch Cultures Limited by Respiration? Journal of Bacteriology* **144,** (1980).
30. Lopatkin, A. J. *et al.* Antibiotics as a selective driver for conjugation dynamics. *Nat. Microbiol.* 16044 (2016). doi:10.1038/nmicrobiol.2016.44